Molecular Therapy
Methods & Clinical Development
Original Article

Lentiviral Hematopoietic Stem Cell Gene Therapy Corrects Murine Pompe Disease

Merel Stok,[1,2,3,9] Helen de Boer,[1,4,10] Marshall W. Huston,[1,5,11] Edwin H. Jacobs,[5,6] Onno Roovers,[1] Trudi P. Visser,[1] Holger Jahr,[7,12] Dirk J. Duncker,[8] Elza D. van Deel,[8,13] Arnold J.J. Reuser,[3,4] Niek P. van Til,[1,14] and Gerard Wagemaker[1,15]

[1]Department of Hematology, Erasmus University Medical Center, Rotterdam, the Netherlands; [2]Department of Pediatrics, Erasmus University Medical Center, Rotterdam, the Netherlands; [3]Center for Lysosomal and Metabolic Diseases, Erasmus University Medical Center, Rotterdam, the Netherlands; [4]Molecular Stem Cell Biology, Department of Clinical Genetics, Erasmus University Medical Center, Rotterdam, the Netherlands; [5]Department of Molecular Genetics, Erasmus University Medical Center, Rotterdam, the Netherlands; [6]Department of Clinical Genetics, Erasmus University Medical Center, Rotterdam, the Netherlands; [7]Department of Orthopaedics, Erasmus University Medical Center, Rotterdam, the Netherlands; [8]Division of Experimental Cardiology, Department of Cardiology, Erasmus University Medical Center, Rotterdam, the Netherlands

Pompe disease is an autosomal recessive lysosomal storage disorder characterized by progressive muscle weakness. The disease is caused by mutations in the acid α-glucosidase (GAA) gene. Despite the currently available enzyme replacement therapy (ERT), roughly half of the infants with Pompe disease die before the age of 3 years. Limitations of ERT are immune responses to the recombinant enzyme, incomplete correction of the disease phenotype, lifelong administration, and inability of the enzyme to cross the blood-brain barrier. We previously reported normalization of glycogen in heart tissue and partial correction of the skeletal muscle phenotype by *ex vivo* hematopoietic stem cell gene therapy. In the present study, using a codon-optimized *GAA* (*GAAco*), the enzyme levels resulted in close to normalization of glycogen in heart, muscles, and brain, and in complete normalization of motor function. A large proportion of microglia in the brain was shown to be GAA positive. All astrocytes contained the enzyme, which is in line with mannose-6-phosphate receptor expression and the key role in glycogen storage and glucose metabolism. The lentiviral vector insertion site analysis confirmed no preference for integration near proto-oncogenes. This correction of murine Pompe disease warrants further development toward a cure of the human condition.

INTRODUCTION

Pompe disease is an autosomal recessive lysosomal storage disorder caused by the deficiency of the lysosomal hydrolase acid α-glucosidase (GAA). GAA deficiency hampers the breakdown of glycogen to glucose and leads to systemic accumulation of glycogen inside the lysosomes.[1–4] The disease manifests as a broad clinical spectrum, ranging from the most severe and rapidly progressive classic infantile form to less progressive forms presenting in late adulthood.[5] Classic infantile Pompe disease presents shortly after birth and is characterized by profound and progressive skeletal muscle weakness, respiratory distress, cardiomyopathy, and death within the first year of life when untreated.[6,7] Patients with classic infantile Pompe disease have an overall better survival and improved quality of life when treated with enzyme replacement therapy (ERT; registered in 2006 as Myozyme, also marketed as Lumizyme), but this therapy has its limitations. Close to 50% of infants still die at a very young age despite ERT, and residual disease remains in the other patients due to insufficient targeting of the skeletal muscles and a neutralizing immune response, particularly in patients that do not produce any endogenous acid GAA.[8–13] Another limitation of ERT is the inability to cross the blood-brain barrier. White matter abnormalities and signs of cognitive decline have been reported in long-term survivors of classic infantile Pompe disease treated with ERT. In mice, signs of CNS involvement and neural deficits have been reported to attribute to respiratory dysfunction.[14–16]

Gene therapy approaches and adjuvant treatments are currently under investigation in preclinical or clinical studies, including the use of adeno-associated viral vectors,[17–19] suppression of autophagy,[20] suppression of glycogen biosynthesis,[21] the use of chaperones,[22,23] and improved ERTs,[24,25] but a single intervention that provides long-

Received 24 January 2020; accepted 27 April 2020;
https://doi.org/10.1016/j.omtm.2020.04.023.

[9]Present address: ProPharma Group, Leiden, the Netherlands

[10]Present address: Merus N.V., Utrecht, the Netherlands

[11]Present address: Sangamo Therapeutics, Richmond, CA, USA

[12]Present address: Department of Orthopaedics, University Hospital RWTH, Aachen, Germany

[13]Present address: Rotterdam University of Applied Sciences, Rotterdam, the Netherlands

[14]Present address: Center for Translational Immunology, University Medical Center Utrecht, the Netherlands, and AvroBio, Cambridge, MA, USA

[15]Present address: Stem Cell Research and Development Center, Hacettepe Medical University, Ankara, Turkey, and Raisa Gorbacheva Memorial Research Institute for Pediatric Oncology and Hematology, First Pavlov State Medical University, Saint Petersburg, Russian Federation

Correspondence: Gerard Wagemaker, Department of Hematology, Erasmus University Medical Center, PO Box 37048, 3005 LA Rotterdam, the Netherlands.
E-mail: g.wagemaker@genetherapy.nl

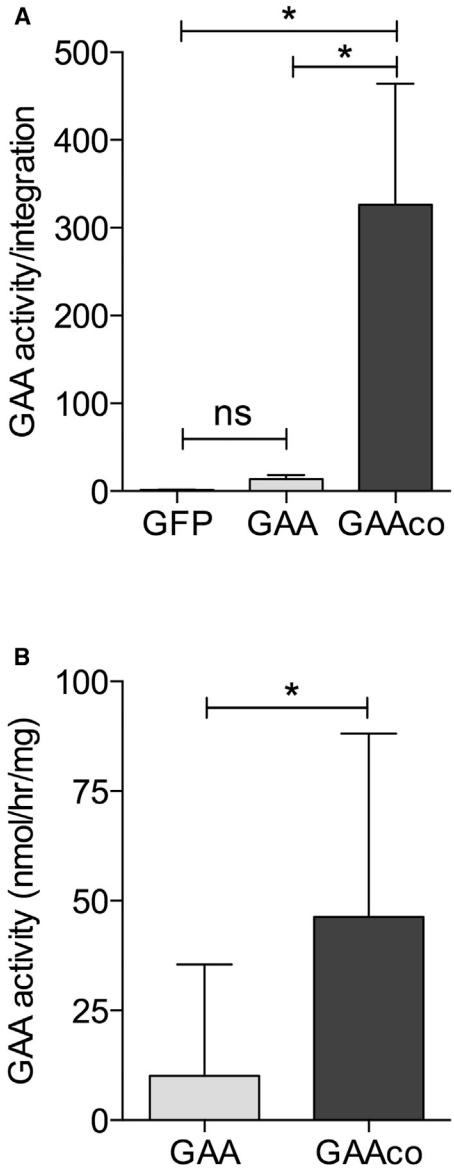

Figure 1. Recoding the GAA Sequence Increases GAA Enzyme Activity per Integration, Resulting in Increased GAA Activity in Leukocytes

(A) *Gaa*$^{-/-}$ mice transplanted with 5 × 10^5 Lin$^-$ cells transduced with either the lentiviral vector expressing the native *GAA* cDNA (GAA), a codon-optimized *GAA* cDNA (GAAco), or *GFP* (control vector; KO), the transgenes driven by the SF promoter and spleen cells collected 10–12 months after transplantation from n = 3 GAA, n = 5 GAAco, and n = 3 KO mice. GAA activity per vector copy number ± SD. (B) GAA activity in leukocytes of individual mice 2 months after transplantation (GAA, n = 10; GAAco, n = 10). Significance was calculated by a Mann-Whitney U test (*p < 0.05).

lasting therapeutic effect with limited risks to develop immune responses against the transgene product is still an unmet medical need.

Transplantation of lentiviral vector gene-modified hematopoietic stem cells (HSCs) has great potential as a delivery tool providing a continuous supply of therapeutic enzyme. Successful clinical trials are currently in progress for X-linked adrenoleukodystrophy (X-ALD) and metachromatic leukodystrophy (MLD).[26,27] As for Pompe disease, we have previously reported a proof of principle that gene-modified HSC transplantation ameliorates the murine Pompe phenotype and results in addition in robust immune tolerance to the transgene product, which is attributable to the intrinsic tolerogenic nature of HSC transplantation.[28] Although sustained elevated GAA levels were achieved, these levels were not sufficiently high to effectuate complete depletion of the accumulated glycogen in skeletal muscle and brain, and to achieve full correction of locomotor function. In the present preclinical evaluation of gene-modified HSC transplantation we explored whether a new vector with codon optimization[29] of the GAA sequence would result in improved reversal of the Pompe disease phenotype.

RESULTS

GAA Enzyme Activities in Blood and Immune Cells

At present, the use of codon-optimized cDNA for improving gene expression is a generally applied and accepted methodology in the development of gene therapeutic approaches. In this study, conducted in GAA-deficient knockout (KO) mice, we have explored a *GAAco* construct using a multiplicity of infection (MOI) of 20 as a potential vector for lentiviral gene therapy in Pompe disease. *GAAco* shares 83% nucleotide sequence identity with the native cDNA, with 422 of the 940 codons modified. Untreated KO animals start to manifest symptoms around 6 months of age but their lifespan is not dramatically shortened.[30] After long-term follow up, i.e., 10–12 months after transplantation, using a study design identical to that published for the GAA construct to allow for a direct comparison,[28] enzyme activity per vector copy in gene-modified spleen cells was increased more than 20-fold by the *GAAco* vector as compared to the *GAA* vector (326.42 ± 307.81 versus 14.4 ± 7.7 nmol/h/mg, respectively; Figure 1). Since the percentage of descendants from the transduced stem cells (i.e., chimerism) was purposely kept at 24.1% ± 5.0% in both groups of mice, the vector copy numbers, as determined by quantitative PCR, were corrected for chimerism and were similar in both groups of mice (*GAAco*, 7.0 ± 2.6; *GAA*, 7.1 ± 5.3). Since enzyme activity per vector copy is independent of cell type and chimerism, the level of chimerism resulted in an overall 4.4-fold increase in leukocytes, thymus, and spleen cells.

Glycogen Clearance in Heart Tissue

Gaa$^{-/-}$ mice present left ventricle hypertrophy and impaired cardiac function, similar to classic infantile Pompe patients. We previously reported that transplantation of KO mice with *GAA*-transduced HSCs reversed heart remodeling and led to a substantial improvement of cardiac function.[28] In the present study we assessed the GAA activity in heart muscle, the cardiac dimensions, and the heart rate at 10 months post-transplantation. Treatment with the lentiviral *GAAco* vector led to an increase of GAA activity in heart 5-fold higher than in wild-type (WT) mice (Figure 2A), resulting in near complete

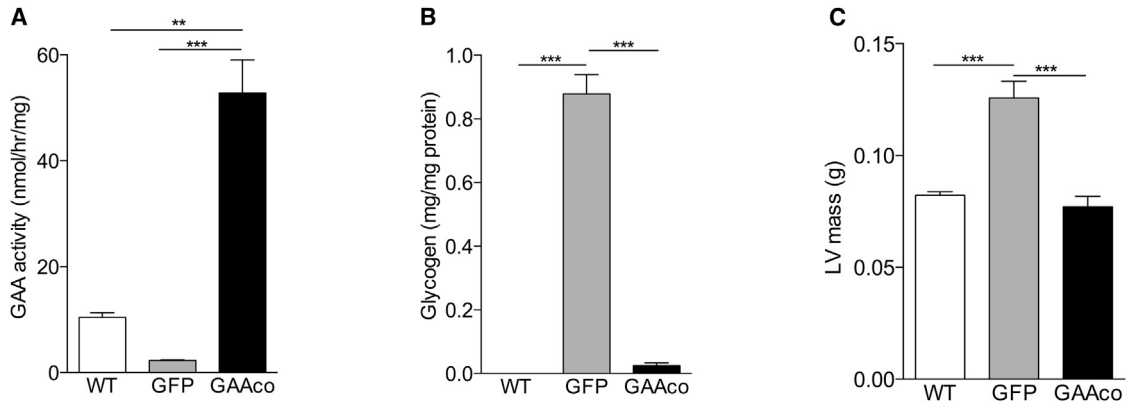

Figure 2. Delivery of High Levels of GAA to Cardiac Tissue Clears Glycogen Storage and Normalizes Cardiac Dimension and Rhythm

(A–C) High enzyme levels were detectable in heart tissue (A), resulting in almost complete reduction of glycogen deposition (B) and normalization of the left ventricular mass in gene therapy-treated mice (C). WT, wild-type animal (n = 3 in biochemical assays, n = 6 in functional tests); GFP, $Gaa^{-/-}$ animals treated with GFP control vector (n = 3–4 in biochemical assays, n = 4–10 in functional tests); GAAco, $Gaa^{-/-}$ animals treated with GAAco vector (n = 5). Data are means of 4–6 mice ± SD. Significance was calculated by a Mann-Whitney U test (*p < 0.05).

normalization of glycogen (Figure 2B). The cardiac hypertrophy present in the untreated $Gaa^{-/-}$ mice normalized in the animals that received HSC-based gene therapy using the *GAAco* cDNA construct (Figure 2C). Normalization of the left ventricular (LV) wall thickness and the LV lumen diameter (data not shown) resulted in a trend to improvement of the heart rhythm (data not shown) and rate (Figure 2D).

Glycogen Clearance in Skeletal Muscle and Normalized Motor Function

$Gaa^{-/-}$ mice at 10 months of age have severely impaired skeletal muscle function. Animals transplanted with *GAAco*-transduced HSCs at age 6–8 weeks had high GAA activity in skeletal muscles when sacrificed 12 months post-transplantation. The muscles studied included tongue, masseter, quadriceps femoris, gastrocnemius, soleus, extensor digitorum longus, and tibialis anterior and displayed near complete reduction of glycogen (Figure 3A). Depending on the particular muscle type, the GAA activity in these muscles was 3- to 40-fold higher than in WT animals, but due to the wide spread between the treated animals there was no significant difference except for the tongue. However, a clear reduction of glycogen can be observed. To investigate the effect on muscle function, the mice were subjected to rotarod and voluntary running wheel tests. Voluntary running wheel activity monitored for 28 days and starting at 10 months post-transplantation displayed no difference between the WT mice and the mice transplanted with *GAAco*-transduced HSCs, whereas *GFP*-transplanted mice ran significantly shorter distances per day (Figure 3B). Dissecting the number of rotations during the 28 days in bins of 2 min demonstrated that the $Gaa^{-/-}$ mice often made fewer rotations than did WT and gene therapy-treated mice (Figure 3C). The distribution of rotations per 2-min bin was very much the same for the *GAAco*-transplanted KO mice and the WT mice, not only in the lower but also in the higher number of rotations per bin. Figure S1 shows actograms of three representative mice from each group, again showing that the *GAAco*-transplanted and WT mice outperform the *GFP*-transplanted mice with regard to daily running wheel activity. Furthermore, the average speed in the running wheels during the 28 days was not different between gene therapy-treated $Gaa^{-/-}$ and WT mice, but untreated $Gaa^{-/-}$ mice reached an average speed around 2-fold lower (Figure 3D). Similarly, *GAAco*-transplanted KO mice managed to stay almost equally long on the accelerating rotarod as did WT mice (Figure 3E), whereas untreated mice fell off rapidly.

Glycogen Clearance in Brain Tissue

A few years after ERT became available for patients with Pompe disease, CNS-related symptoms were revealed. It is well accepted that hematopoietic stem cell transplantation (HSCT) can alleviate neurological symptoms of lysosomal enzyme deficiencies by contributing to the pool of enzyme-expressing microglia that resides in the brain.[26,31,32] Transplantation of $Gaa^{-/-}$ mice with the *GAAco* construct-transduced HSCs led to a significant increase of GAA activity to a level of approximately half that in brain of WT mice (Figure 4A), resulting in reduction of glycogen to near normal levels (Figure 4B), with glycogen staining largely restricted to astrocytes (Figure 4C).

To display the localization of GAA in detail, we performed immunofluorescence staining of brain sections from mice 3.5 months post-transplantation, which demonstrated GAA in roughly half of the microglia and in virtually all astrocytes (Figure 5).

Glycogen Clearance in Visceral Organs and Articular Cartilage

Since glycogen deposition occurs in virtually all tissues, visceral organs were measured for enzyme activity and glycogen content. High enzyme activity was also detected in these organs (i.e., liver and kidney), and with full glycogen clearance (Figure 6).

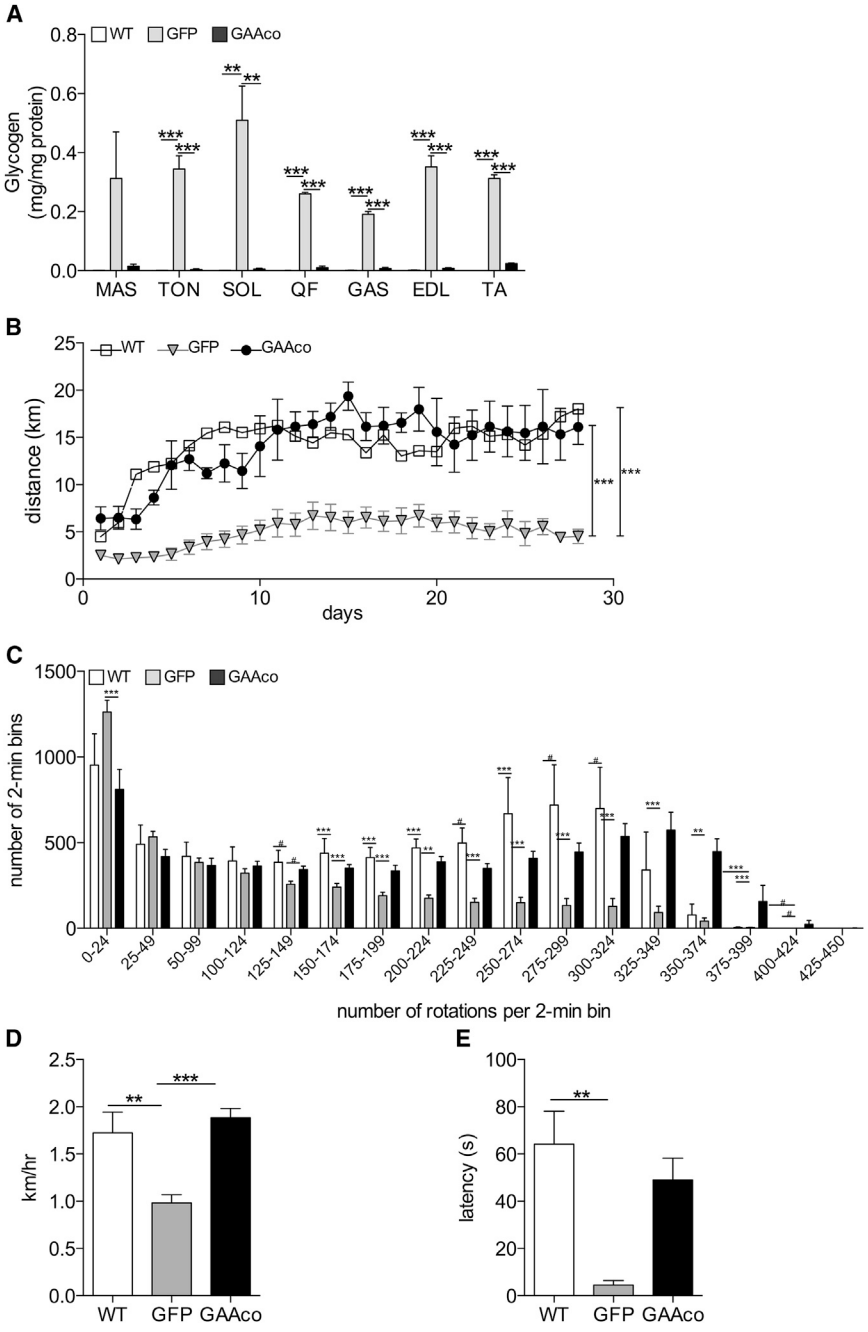

Figure 3. GAA Expression Clears Glycogen Storage and Corrects Skeletal Muscle Function

(A) Near complete reduction of glycogen content in the skeletal muscles (masseter) (MAS), tongue (TON), soleus (SOL), quadriceps femoris (QF), gastrocnemius (GAS), extensor digitorum longus (EDL), and tibialis anterior (TA). Number of mice per group: WT, n = 3–5; GAAco, n = 4–5; GFP, n = 3–5. Rotarod and running wheel performance was determined at 10–12 months post-transplantation and compared to age-matched WT and GFP controls. (B) Distance achieved in a voluntary running wheel. Number of mice per group: WT, n = 3; GAAco, n = 4; GFP, n = 9. (C) The number of rotations made in the running wheel was measured in 2-min bins, categorized in 17 levels of performance, and the frequency per category was scored during a period of 28 days. (D) Performance of mice on a rotarod. Latency indicates the time spent on the rotarod before falling off. Number of mice per group: WT, n = 6; GAAco, n = 5; GFP, n = 4. (E) Average speed in the running wheel. Data are means ± SD and significance was calculated with a Mann-Whitney U test (*$p < 0.05$, **$p < 0.01$, ***$p < 0.001$).

Cells residing in articular cartilage may be difficult to reach by GAA due to its impenetrable density and low oxygenation from virtually no blood supply. Chondrocytes residing in tibio-femoral joint cartilage of Pompe mice were subjected to periodic acid-Schiff (PAS) staining (Figure 7). Quantification, with the PAS staining intensity of WT chondrocytes set at 0%, demonstrated that ~93% of the chondrocytes were glycogen positive in KO mice, which was reduced to ~45% positive cells in *GAAco*-treated animals. In addition to increased PAS staining intensity, we noted chondrocyte hypertrophy in the articular cartilage of KO mice, whereas the cartilage of *GAAco*-treated mice appeared morphologically normal compared to age-matched WT mice.

Vector Integration Site Analysis and Safety Profiling

Bone marrow DNA from five KO mice transplanted with *GFP*-transduced HSCs and 36 KO mice transplanted with *GAAco*-transduced HSCs were used as a template for linear amplification-mediated PCR (LAM-PCR) reactions prior to high-throughput sequencing. A total of 757 unique integration sites were mapped to the murine genome: 424 in the DNA from mice transplanted with the *GFP* vector, and 333 in the DNA from mice transplanted with the *GAAco* vector. Hits were widely distributed across the genome (Figure 8A), and integrations were annotated to the gene with the nearest transcription start site. Using this approach, the genes nearest to each integration site were sorted into 10 bins based on their expression levels in lineage-negative (Lin^-) Sca-1^+ c-Kit^+ (LSK) bone marrow cells, with genes in the higher expression bins being favored for integration (Figure 8B).

Integration site genes were screened against a list of 528 oncogenes compiled by the Retroviral Tagged Cancer Gene Database (RTCGD) database.[33] Fifteen oncogenes were found in the annotation of the integration sites in *GAAco*-treated mice (4.2% of the sample pool), with two oncogenes appearing twice, i.e., *Cr2* and *Eps15l1*. This percentage is similar to the frequency of integrations near oncogenes

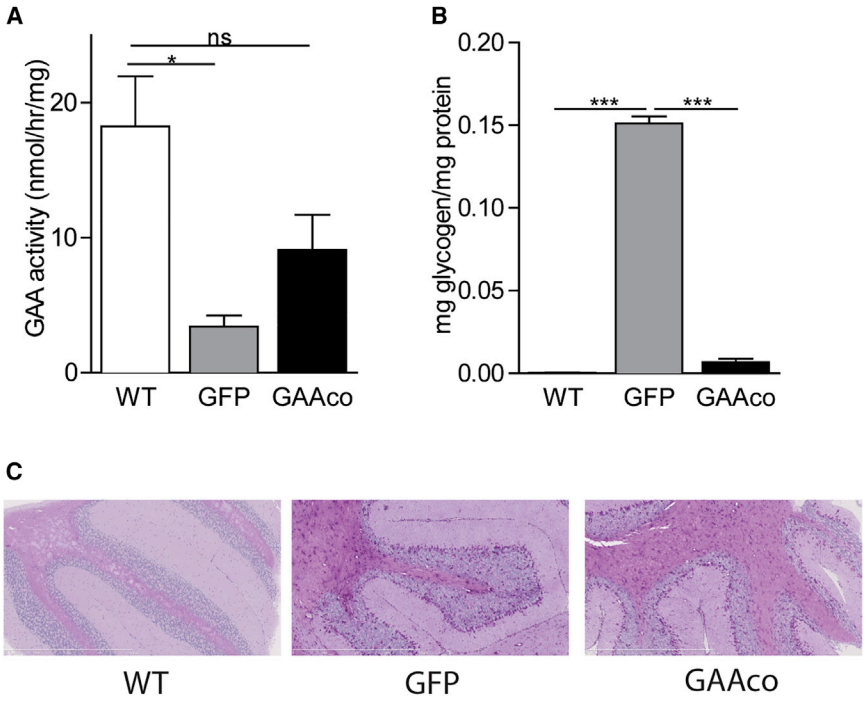

Figure 4. Enzyme Activity and Glycogen Levels in Brain Tissue

(A and B) GAA activity (A) and glycogen content (B) in whole-brain lysates, 12 months after transplantation. Data are expressed as mean ± SD. Number of mice per group: WT, n = 3; GAAco, n = 5; GFP, n = 3. (C) PAS staining of cerebellum, demonstrating selective storage of glycogen in astrocytes and residual glycogen in astrocytes of gene therapy-treated mice. Significance was calculated with a Mann-Whitney U test (*$p < 0.05$).

found in *in vivo* studies of WT murine Lin^- cells transduced with *GFP* (58 of 1,402, amounting to 4.1%, with oncogene *Zfp521* appearing twice), and close to the frequency expected by random chance (528 oncogenes out of 21,886 RefSeq genes in Ensembl, amounting to 2.5% oncogene frequency in the murine genome). Fifteen genes were annotated three or more times in the *GAAco*-treated group and 25 genes in the *GFP*-treated group, and these can be considered common integration sites (CISs) (Tables S1 and S2). Most of the common integration sites were intronic, and none of the CIS genes was marked as oncogenes or present in the two highest LSK expression bins.

DISCUSSION

ERT for Pompe disease is not curative and is only partially effective, requires weekly or biweekly enzyme infusions, may result in neutralizing immune responses to the recombinant enzyme, and is very expensive. The most severely affected cross-reactive immunologic material (CRIM)-negative Pompe patients still have a strongly reduced overall survival, a need for respiratory support, and develop high antibody titers against the recombinant protein. Hence, a single intervention with curative intent represents an unmet medical need.

Attempts at gene therapy in Pompe disease include adeno-associated virus (AAV) through *in vivo* injections, or using lentiviral vectors, and *ex vivo* lentiviral transduction of HSCs.[17,19,28,34–37] Although AAV therapy may correct disease in Pompe mice, and potentially provide partial reduction of glycogen in brain when secretable GAA fusion proteins are used, to correct Pompe patients would require a large AAV vector quantity, which poses a risk of immune responses against the transgene product and/or AAV capsid.[19] In a previous report we showed that gene-modified HSCs provided immune tolerance to GAA, and that this approach ameliorates the Pompe phenotype.[28] Supranormal enzyme levels were obtained in hematopoietic cells, and most target tissues reached enzyme activity similar to that of WT mice. However, skeletal muscle function was not fully normalized, and an effect on glycogen levels in brain tissue was absent. The present study is based on the hypothesis that codon optimization of the GAA sequence might result in enzyme levels sufficient for full correction of the Pompe phenotype. The self-inactivating (SIN) third-generation lentiviral vector used in this study contained the strong spleen focus-forming virus (SFFV) viral promoter driving *GAAco* expression. Recoding *GAA* resulted on average in a 20-fold increase of the acid GAA activity per viral copy number (VCN) in spleen, which also resulted in increased enzyme activities in target tissues, near complete reduction of glycogen to WT levels, and consequently normalized heart parameters and function in the gene therapy-treated mice as well as locomotor function in voluntary running wheels and rotarod tests. The increase of GAA activity in skeletal muscles resulted in a near complete reduction of glycogen shown in Figure 3A, which ultimately led to a normalization of skeletal muscle function (Figures 3B–3E).

Despite prominent glycogen storage in brain tissue, Pompe disease, in contrast to most other lysosomal enzyme deficiencies, does not result in prominent neurological symptoms. However, some signs of CNS deficits became apparent in classic infantile patients treated with ERT.[14,38] In addition, neural deficits in Pompe mice may contribute to respiratory insufficiency[39–41] and even skeletal muscle dysfunction.[42] GAA is thought not to pass the blood-brain barrier, so ERT is not expected to have any effect on glycogen levels in the brain, but gene therapy approaches may, which require further investigation. We previously established in the Krabbe mouse model that monocytes pass the blood-brain barrier to contribute to microglia and thereby deliver the needed enzyme.[43] Based on this rationale, gene-modified HSCs are used successfully in lentiviral clinical trials for X-ALD and MLD to counteract the neuronal damage, including cognitive decline.[26,44] Using the *GAA* lentiviral vector, GAA levels

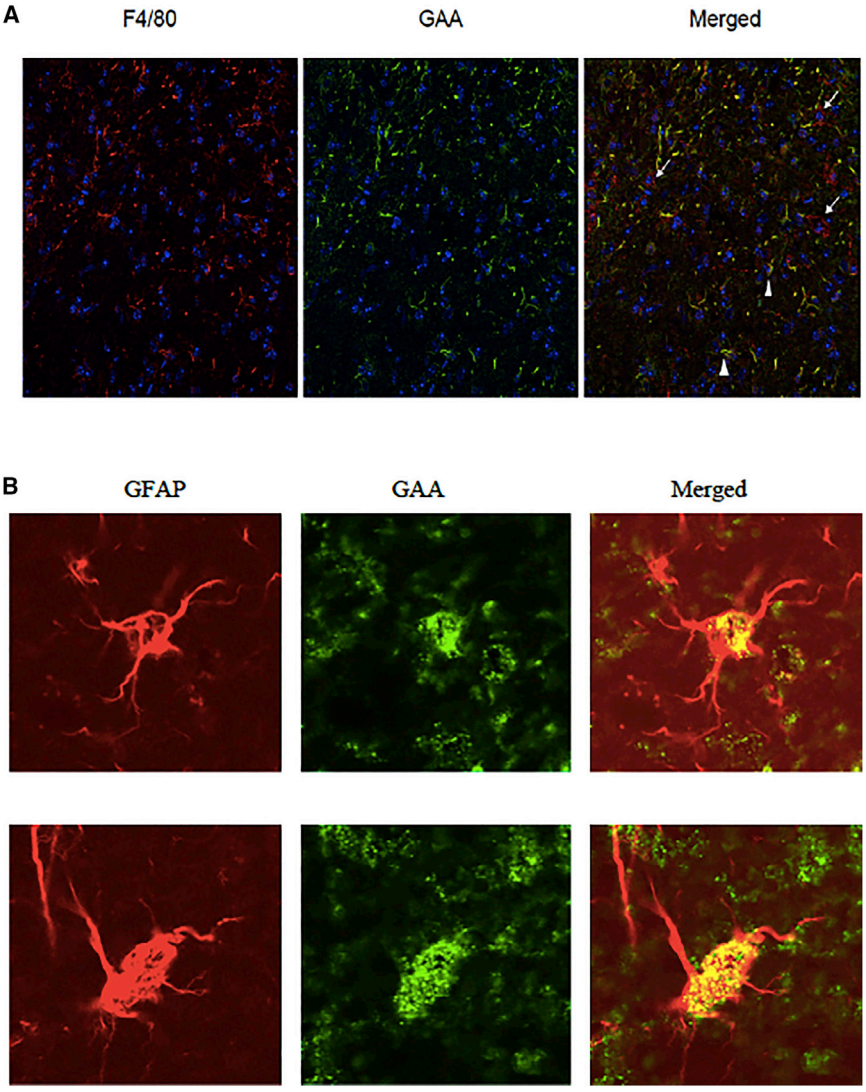

Figure 5. GAA in Microglia and Astrocytes

(A) Microglia (F4/80, left panel); anti-GAA and Hoechst staining show that around half of microglia are GAA positive (arrowheads) and show the presence of GAA-negative resident microglia (arrows); original magnification, ×20. (B) Virtually all astrocytes appeared to contain GAA protein; two representative examples are shown here. The merged panel of the GFAP and GAA staining demonstrates the localization of GAA; original magnification, ×100. Figure S2 shows the reverse magnifications for microglia and astrocytes, respectively.

were very low in brain without much effect on glycogen, but using the vector described in the present study, glycogen levels were reduced close to WT levels, in accordance with a GAA level approximately half that of normal mice. As for the mechanism, approximately half of the microglia appeared to contain GAA and are therefore descendants of transduced stem cells, whereas the resident microglia or the untransduced donor microglia did not display GAA. This finding is consistent with a population of resident microglia, which originate from early yolk sac precursors prior to birth and persist throughout life, and microglia derived from monocytes infiltrating the brain in response to tissue damage or inflammation.[45–47]

Somewhat surprisingly, virtually all astrocytes appeared to contain GAA. Astrocytes have emerged as major players in energy delivery, production, utilization, and storage of the brain and almost exclusively store glycogen, as was also observed in the present study and most likely explains the limited neurological symptoms in the Pompe disorder in contrast to most other lysosomal enzyme deficiencies. Astrocytes play a major role in development, maintenance, and modulation of the blood-brain barrier, control energy supply, in particular through the glucose metabolism and specific neuronal capacities such as long-term memory, and express the mannose 6-phosphate receptors by which GAA is internalized,[48–50] which explains why virtually all astrocytes appeared GAA positive after treatment by the gene-modified HSC approach. Such a reduction of the total glycogen content of the brain should contribute to an improved overall outcome following gene therapy in classic infantile patients. Interestingly, the efficacy of our approach was also apparent in a major reduction in intracellular glycogen accumulation in articular cartilage despite the fact that chondrocytes are particularly difficult to target due to the composition and density of the surrounding matrix.

The present results were obtained using the strong gammaretroviral SFFV promoter and a relatively high VCN per cell (an average of 7 VCN per cell) and are in line with the high doses of ERT required to alleviate the Pompe phenotype. In a follow-up study we have been able to reduce the VCN required to 1–2 per cell by glycosylation-independent lysosomal targeting[24,51] (unpublished data).

The initial stem cell gene therapy trials for X-linked severe combined immune deficiency (SCID) using gammaretroviral gene transfer vectors resulted in successful restoration of T cell immunity, but, unfortunately, in six patients autonomous T cell clones developed into leukemia, among which one patient did not survive. However, it has meanwhile been recognized that the treated immune deficiency disorders at least co-predispose to leukemia development, given the absence of leukemia in the adenosine deaminase-deficient (ADA)-SCID trial,[52,53] a 30% incidence in the X-linked SCID trials,[54–56] and a 90% incidence in the gammaretroviral Wiskott-Aldrich trial.[57]

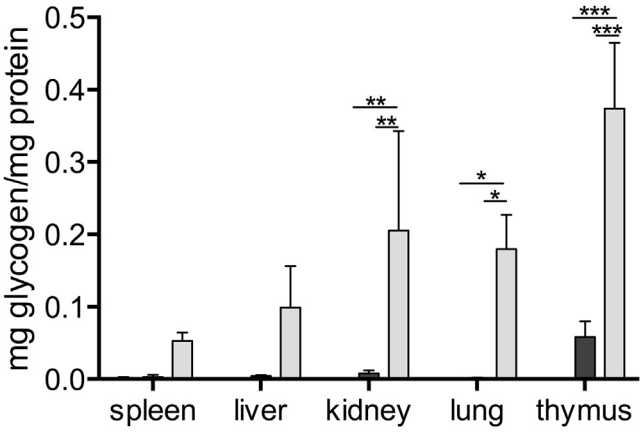

Figure 6. Reduction of Glycogen Storage in Visceral Organs

Glycogen values determined in visceral organs at 10–12 months after transplantation of gene-modified cells; data are expressed as mean ± SD. Age-matched *Gaa*$^{-/-}$ (KO) and wild-type (WT) animals were used as controls; n = 4–10 mice. Statistical analysis was calculated with a Mann-Whitney U test (*p < 0.05).

Of note, no such adverse effects occurredd in any preclinical evaluation or clinical trial of enzyme deficiencies, including ADA-SCID, which, although listed as a primary immune deficiency, is in essence a systemic enzyme deficiency. Safety issues of the gammaretroviral vectors have been improved by third-generation lentiviral vectors made SIN by deletion of enhancer regions from the long terminal repeat sequences[58–60] to reduce the risk of influencing nearby genes,[61] resulting in highly favorable safety profiles, as is also encountered in the analysis of vector integration sites in Pompe mice, which showed the expected lentiviral vector integration pattern. A more thorough comparison of lentiviral vector integration site distributions by vectors containing viral and eukaryotic promoters, various therapeutic transgenes and used in different species (unpublished data) showed no significantly increased risk of the strong SFFV promoter in integration frequency near oncogenes compared to eukaryotic promoters. Also, genotoxic events were absent during prolonged monitoring of mice transplanted with stem cells transduced with the *GFP* or *GAAco* vectors.

The present report demonstrates that transplantation of mice at 6–8 weeks of age with HSCs transduced using a highly efficient overnight gene transfer method with a third-generation SIN lentiviral vector containing a codon-optimized transgene driven by the strong SFFV promoter results in high and sustained GAA activity in the tissues that are most affected in Pompe disease. Consequently, biochemical and functional parameters of heart and skeletal muscle tissues normalized, and, in addition, glycogen accumulation in the brain appeared to be reduced to near normal levels. Serious adverse effects were not observed during prolonged monitoring of the treated animals, resulting in a favorable safety profile confirmed by the integration analysis. The therapeutic findings warrant further development including similar, better, and/or safer constructs directed at clinical implementation of the approach as a single intervention therapy with curative intent. Patients with classic infantile and juvenile Pompe disease are presently seen as the first target group because of their relative resistance to the negative side effects of bone marrow transplantation and their upcoming severe pathology when treated with ERT, whereas late-onset Pompe disease requires further consideration and a specific risk/benefit analysis.

MATERIALS AND METHODS

Animals

Gaa$^{-/-}$ mice (FVB/N background) were generated as previously described.[62] Age-matched control female FVB/N mice (WT) were obtained from Charles River Nederland (Maastricht, the Netherlands) and used as controls. All procedures for this study were approved by the Animal Ethics Committee of the Erasmus University Medical Center, Rotterdam in accordance with legislation in the Netherlands.

Construction of Vector Plasmids

The human *GAA* native construct driven under the SFFV promoter has been described previously (pRRL.PPT.SFFV.GAA.bPRE4*.SIN [GAA]).[28] The OptimumGene algorithm and synthesis were performed by GenScript (Piscataway, NJ, USA) to optimize the human *GAA* open reading frame for improved expression, including consensus Kozak sequence and an additional TGA stop codon (*GAAco*). *GFP* in the pRRL.PPT.SFFV.GFP.bPRE4*.SIN vector (referred to as *GFP*) was replaced by *GAAco,* creating the pRRL.PPT.SFFV.GAAco.bPRE4*.SIN vector (referred to as *GAAco*).

Transduction and Transplantation of Murine HSCs

Bone marrow was harvested from the femora and tibiae of 8- to 12-week-old male *Gaa*$^{-/-}$ mice. Lin^{-} cells were purified using a mouse HSC isolation kit (BD Biosciences) and transduced with the *GAAco* vector at an MOI of 20 (mice are marked as GAAco) and an MOI of 2 for the *GFP* vector, the latter to serve for mock therapy (these mice are marked as GFP). Cells were transduced overnight in serum-free enriched Dulbecco's medium, supplemented with murine stem cell factor (100 ng/mL), human FMS-like tyrosine kinase 3 murine ligand (50 ng/mL), and murine thrombopoietin (10 ng/mL), as previously described.[63] Transduced cells (5×10^5 cells) were transplanted via the tail vein of 6- to 8-week-old *Gaa*$^{-/-}$ female recipients after sublethal irradiation (6 Gy).

Muscle Performance Tests

To determine skeletal muscle function, mice were tested at 12 months after transplantation on an accelerating rotarod (from 4 to 40 rpm in 5 min; Panlab/Harvard Apparatus Rota Rod, Holliston, MA, USA). Mice were given two training sessions to adjust to the apparatus, followed by three runs with an interval of 5 min, and the average latency to fall from the rotarod was determined.

The distance run voluntarily in a running wheel was used to measure activity performance at 10 months after transplantation for 28 days. Mice were individually housed in type III polyester cages, equipped with a steel running wheel (diameter 11.8 cm) connected to a sensor system to detect revolutions of the wheel.[64] Running wheel activity

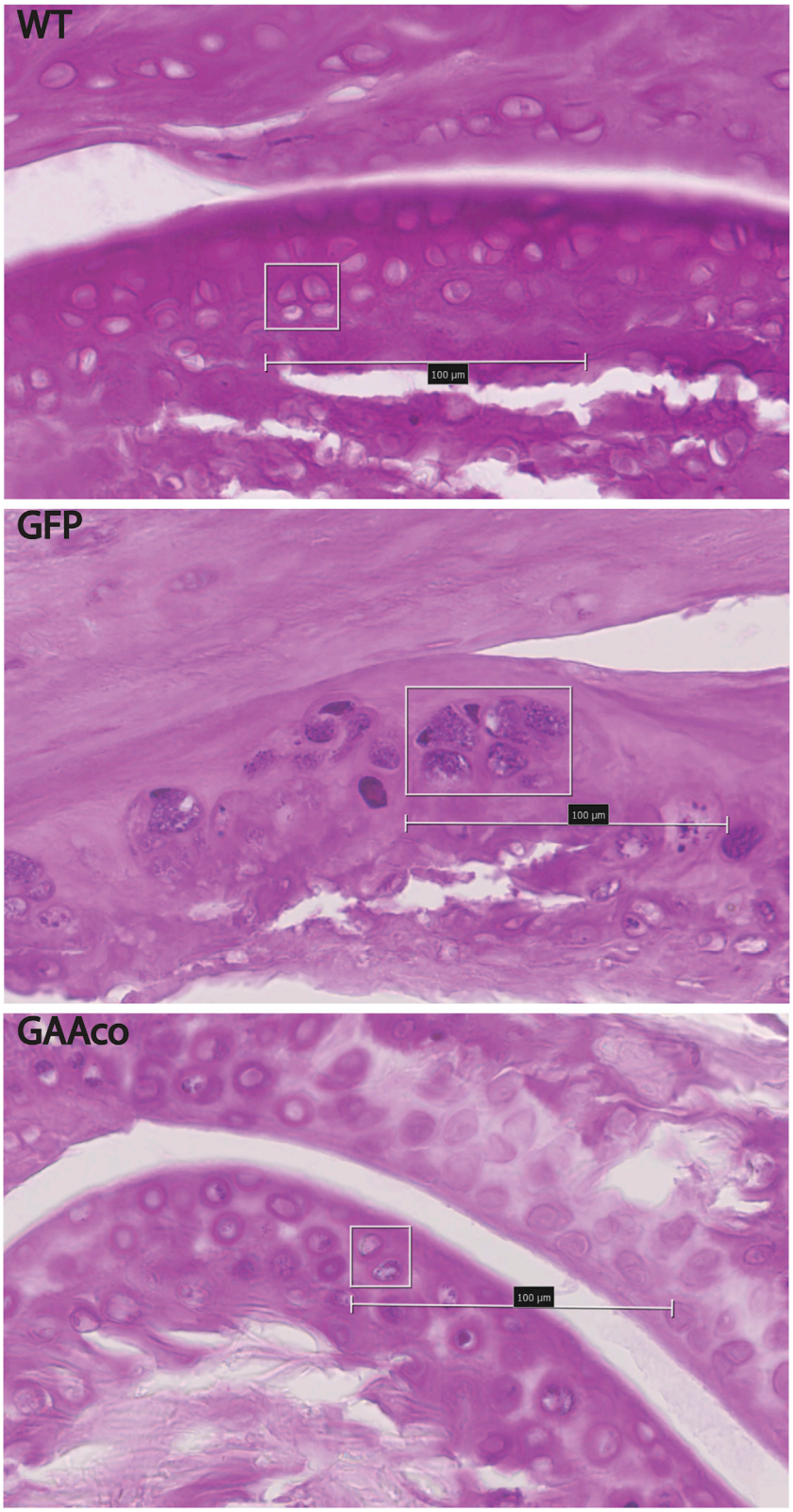

Figure 7. Clearance of Glycogen in Articular Cartilage after Gene Therapy Treatment

PAS staining (dark purple granules) of articular cartilage shows glycogen storage in approximately 93% of the chondrocytes of 10-months-old GAA-deficient (GFP) mice. The GAAco (treated mice (GAAco, bottom panel) show a reduction in the number of PAS-positive chondrocytes to approximately 45%, as well as in the intensity of the PAS staining. Wild-type mice (WT, top panel) have no glycogen storage detetctable by PAS staining. Original magnification, ×40; scale bars represent 100 µm.

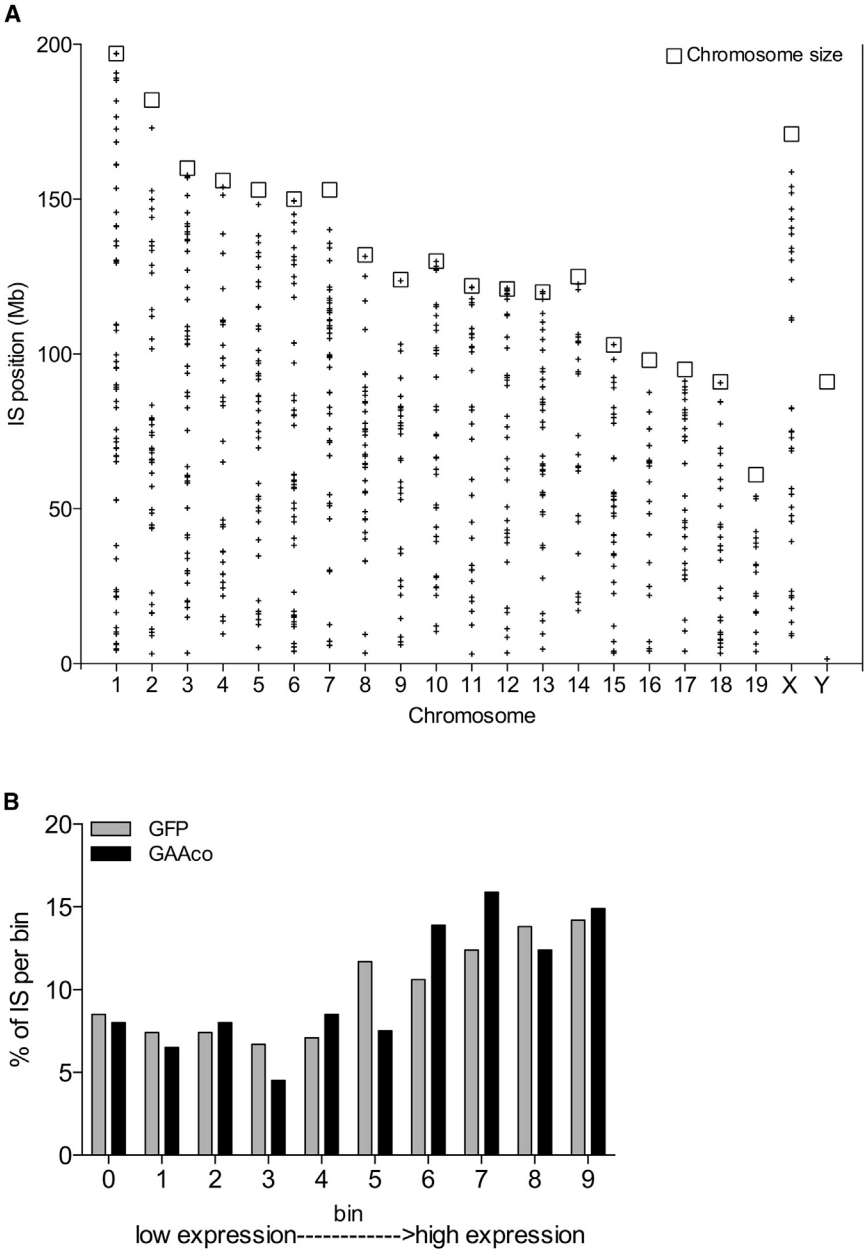

Figure 8. Vector Integration Analysis of Bone Marrow of Gene Therapy-Treated Mice

(A) Distribution of the retrieved lentiviral integrations on each chromosome of *GAAco*-treated mice, 10–12 months after transplantation. (B) The expression of the nearest gene to the vector integration site was assigned a bin from low to high expression. Both integrations of *GFP*- and *GAAco*-transduced bone marrow are presented. The vector integrations show the expected lentiviral vector distribution with more frequent integrations in the higher expression bins.

(number of revolutions per 2 min) was continuously recorded using the ERS program (University of Groningen, Groningen, the Netherlands). The daily distance that the mice ran was calculated by multiplying the number of revolutions with the circumference of the wheels. The average running speed was calculated for the time that the mice spent in the running wheel.

Tissue Preparation and Histology

At 12 months post-transplantation, the mice were fasted overnight and sacrificed by transcardial perfusion with saline after sedation with ketamine/Sedator mix (Eurovet Animal Health Limited, Bladel, the Netherlands). Tissues were collected and homogenized by TissueLyser II (QIAGEN) twice for 2.5 min at 30 Hz. Histological assessment was performed as described earlier.[31] PAS (for glycogen) staining was performed on these slides as previously described with the exception of cartilage. The tibialis bones were collected and undecalcified and embedded in methyl methacrylate (MMA). Positive PAS chondrocytes were counted and displayed as percentages of total chondrocytes.

Immunofluorescence Staining

For localization of GAA in the brain, transplanted mice were overnight fasted and sacrificed by transcardial perfusion with saline followed by 4% formaldehyde (FA) in phosphate-buffered saline (PBS) after administration of a ketamine/Sedator mix, 3.5 months after transplantation (n = 3). The entire brain was dissected out and overnight fixed in 4% FA before being frozen in OCT Tissue Tek (Sakura Finetek Europe). Sections were permeabilized in acetone and methanol (1:4 [v/v]) prior to blocking in 10% fetal calf serum in PBS at room temperature, and subsequently stained for GAA (anti-GAA 1:100), anti-glial fibrillary acidic protein (GFAP; Sigma-Aldrich; 1:500), and F4/80 (AbD Serotec; 1:200) overnight at 4°C. The following secondary antibodies were used: Alexa Fluor 488/555/647 (Invitrogen; 1:500). Hoechst (Sigma-Aldrich; 1:15,000) was used for nuclear staining. Tissue sections were examined by fluorescence microscopy (Leica DMRXA) connected to a Leica DFC 350FX camera.

GAA and Glycogen Assays

GAA activity and glycogen content were determined as described previously[64,65] and corrected for protein content (bicinchoninic acid [BCA] kit, Pierce). The glycogen content shown in Figures 3 and 7 were obtained using undiluted samples, which may maximally result in a factor 2 lower compared to the results from titrated samples,

however irrelevant for the conclusion of correction of glycogen in the tissues involved.

Quantitative PCR of LV Integrations

Spleen DNA was extracted with the NucleoSpin tissue kit (Bioké). To determine the vector copies per cell, quantitative PCR was performed on DNA extracted from spleen cells with HIV-ΔU3 forward primer (5′-CTGGAAGGGCTAATTCACTC-3′) and HIV-PSI reverse primer (5′-GGTTTCCCTTTCGCTTTCAG-3′) on the ABI Prism 7900 HT sequence detection system (Applied Biosystems). To determine the chimerism, Y chromosome-specific *Sry* locus primers were used: forward, 5′-CATCGGAGGGCTAAAGTGTCAC-3′, reverse 5′-TGGCATGTGGGTTCCTGTCC-3′. Samples were normalized to mouse *Gapdh* (forward primer, 5′-CATCACTGCCACCCAGAAGAC-3′, reverse primer, 5′-TGACCTTGCCCACAGCCTTG-3′). Samples were analyzed with SDS 2.2.2 software (Applied Biosystems).

LAM-PCR

High-resolution insertion-site analysis by LAM-PCR[66] was performed on bone marrow DNA of $Gaa^{-/-}$ mice transduced with SF.*GFP* (n = 5) or SF.*GAAco* (n = 36) LV vectors. Restriction enzyme Tsp509I was used with the lentiviral (HIV) primer set, and PCR products were run on high-resolution polyacrylamide (Spreadex) gel. Sequencing reads were analyzed using MAVRIC,[67] and to obtain the nearest RefSeq gene, the following settings were used: no repeat masking; minimum sequence length, 20 bp; minimum BLAST e-value, 0.01; and maximum distance from integration site to look for genes, 100 kb. Sequences were aligned to the murine genome via BLAST (v.37) and nearby genes identified using Ensembl version 59.

Echocardiography

Ten months after transplantation, mice were weighed, anesthetized with isoflurane, and intubated as previously described.[68] Animals were placed on a heating pad to maintain body temperature at 37°C while being artificially ventilated with a mixture of O_2 and N_2 (1:2 [v/v]) to which isoflurane (2.5% [v/v]) was added at a rate of 90 strokes/min using a rodent ventilator (SAR-830/P, CWE, Ardmore, PA, USA) at an inspiratory pressure of 18 cm H_2O and a positive end expiratory pressure of 4 cm H_2O. To dehair the chest, Veet hair removal cream (Reckitt Benckiser, Parsippany, NJ, USA) was used. Transthoracic echocardiograms of the left ventricle were obtained with an Aloka SSD 4000 echo device (Aloka, Tokyo, Japan) using a 13-MHz probe. Images of the short and long axes were obtained in two-dimensional and M-mode settings, used to measure the LV lumen diameter and wall thickness at end diastole and end systole by SigmaScan Pro 5 image analysis software.

Statistical Analysis

Statistical analysis was performed with GraphPad Prism (GraphPad, La Jolla, CA, USA). Significance of differences was determined by the Mann-Whitney U test. A significant difference was assumed at $p < 0.05$. Error bars represent SD, as indicated in the legends.

SUPPLEMENTAL INFORMATION

Supplemental Information can be found online at https://doi.org/10.1016/j.omtm.2020.04.023.

AUTHOR CONTRIBUTIONS

M.S. contributed to the design of experimental work, executed most of the technical work, designed figures, interpreted data, and contributed to writing the manuscript; H.d.B, T.P.V., O.R., H.J., and E.D.v.D. performed technical work and interpreted data; M.W.H. and E.H.J. executed technical work, interpreted data, and contributed to the manuscript; A.J.J.R. and N.P.v.T. contributed to experimental design, interpretation of data, and the manuscript; and G.W. designed the project and contributed to the experimental design, interpretation of data, and writing the manuscript.

CONFLICTS OF INTEREST

The authors declare no competing interests.

ACKNOWLEDGMENTS

The authors gratefully acknowledge Ton de Jong and Nicole Kops for assistance with histochemistry. This work was supported by the European Commission's 5th, 6th, and 7th Framework Programs (contracts QLK3-CT-2001-00 427-INHERINET and LSHB-CT-2004-005242-CONSERT and grant agreement no. 222878-PERSIST); the Netherlands Organization for Health Research (ZonMw) (program grant 434-00-010); and by the Netherlands Organisation for Scientific Research (NWO) (project 021.002.129). E.H.J. received support from the the Netherlands Organisation for Scientific Research (NWO) ZonMw-Veni award (40-00806-98-06082) and the European Research Advisory Board (ERAB) project grant EA 07 14.

REFERENCES

1. van der Ploeg, A.T., and Reuser, A.J. (2008). Pompe's disease. Lancet *372*, 1342–1353.
2. Hagemans, M.L., Winkel, L.P., Van Doorn, P.A., Hop, W.J., Loonen, M.C., Reuser, A.J., and Van der Ploeg, A.T. (2005). Clinical manifestation and natural course of late-onset Pompe's disease in 54 Dutch patients. Brain *128*, 671–677.
3. Hirschhorn, R. (2001). Glycogen storage disease type II: acid alpha-glucosidase (acid maltase) deficiency. In The Metabolic and Molecular Bases of Inherited Disease, *Volume III*, Eighth Edition., C. Scriver, A.L. Beaudet, W.S. Sly, and D. Valle, eds. The Metabolic and Molecular Bases of Inherited Disease (McGraw-Hill), pp. 3389–3420.
4. Winkel, L.P., Hagemans, M.L., van Doorn, P.A., Loonen, M.C., Hop, W.J., Reuser, A.J., and van der Ploeg, A.T. (2005). The natural course of non-classic Pompe's disease; a review of 225 published cases. J. Neurol. *252*, 875–884.
5. Güngör, D., and Reuser, A.J. (2013). How to describe the clinical spectrum in Pompe disease? Am. J. Med. Genet. A. *161A*, 399–400.
6. Noordzij, J.G., Verkaik, N.S., van der Burg, M., van Veelen, L.R., de Bruin-Versteeg, S., Wiegant, W., Vossen, J.M., Weemaes, C.M., de Groot, R., Zdzienicka, M.Z., et al. (2003). Radiosensitive SCID patients with Artemis gene mutations show a complete B-cell differentiation arrest at the pre-B-cell receptor checkpoint in bone marrow. Blood *101*, 1446–1452.
7. van den Hout, H.M., Hop, W., van Diggelen, O.P., Smeitink, J.A., Smit, G.P., Poll-The, B.T., Bakker, H.D., Loonen, M.C., de Klerk, J.B., Reuser, A.J., and van der Ploeg, A.T. (2003). The natural course of infantile Pompe's disease: 20 original cases compared with 133 cases from the literature. Pediatrics *112*, 332–340.
8. van Capelle, C.I., Winkel, L.P., Hagemans, M.L., Shapira, S.K., Arts, W.F., van Doorn, P.A., Hop, W.C., Reuser, A.J., and van der Ploeg, A.T. (2008). Eight years experience

with enzyme replacement therapy in two children and one adult with Pompe disease. Neuromuscul. Disord. *18*, 447–452.

9. Strothotte, S., Strigl-Pill, N., Grunert, B., Kornblum, C., Eger, K., Wessig, C., Deschauer, M., Breunig, F., Glocker, F.X., Vielhaber, S., et al. (2010). Enzyme replacement therapy with alglucosidase alfa in 44 patients with late-onset glycogen storage disease type 2: 12-month results of an observational clinical trial. J. Neurol. *257*, 91–97.

10. Kishnani, P.S., Corzo, D., Leslie, N.D., Gruskin, D., Van der Ploeg, A., Clancy, J.P., Parini, R., Morin, G., Beck, M., Bauer, M.S., et al. (2009). Early treatment with alglucosidase alpha prolongs long-term survival of infants with Pompe disease. Pediatr. Res. *66*, 329–335.

11. van Capelle, C.I., van der Beek, N.A., Hagemans, M.L., Arts, W.F., Hop, W.C., Lee, P., Jaeken, J., Frohn-Mulder, I.M., Merkus, P.J., Corzo, D., et al. (2010). Effect of enzyme therapy in juvenile patients with Pompe disease: a three-year open-label study. Neuromuscul. Disord. *20*, 775–782.

12. van der Ploeg, A.T., Clemens, P.R., Corzo, D., Escolar, D.M., Florence, J., Groeneveld, G.J., Herson, S., Kishnani, P.S., Laforet, P., Lake, S.L., et al. (2010). A randomized study of alglucosidase alfa in late-onset Pompe's disease. N. Engl. J. Med. *362*, 1396–1406.

13. van der Ploeg, A.T. (2010). Where do we stand in enzyme replacement therapy in Pompe's disease? Neuromuscul. Disord. *20*, 773–774.

14. Ebbink, B.J., Poelman, E., Plug, I., Lequin, M.H., van Doorn, P.A., Aarsen, F.K., van der Ploeg, A.T., and van den Hout, J.M. (2016). Cognitive decline in classic infantile Pompe disease: an underacknowledged challenge. Neurology *86*, 1260–1261.

15. Gambetti, P., DiMauro, S., and Baker, L. (1971). Nervous system in Pompe's disease. Ultrastructure and biochemistry. J. Neuropathol. Exp. Neurol. *30*, 412–430.

16. Fuller, D.D., ElMallah, M.K., Smith, B.K., Corti, M., Lawson, L.A., Falk, D.J., and Byrne, B.J. (2013). The respiratory neuromuscular system in Pompe disease. Respir. Physiol. Neurobiol. *189*, 241–249.

17. Sun, B., Zhang, H., Bird, A., Li, S., Young, S.P., and Koeberl, D.D. (2009). Impaired clearance of accumulated lysosomal glycogen in advanced Pompe disease despite high-level vector-mediated transgene expression. J. Gene Med. *11*, 913–920.

18. Mah, C., Pacak, C.A., Cresawn, K.O., Deruisseau, L.R., Germain, S., Lewis, M.A., Cloutier, D.A., Fuller, D.D., and Byrne, B.J. (2007). Physiological correction of Pompe disease by systemic delivery of adeno-associated virus serotype 1 vectors. Mol. Ther. *15*, 501–507.

19. Puzzo, F., Colella, P., Biferi, M.G., Bali, D., Paulk, N.K., Vidal, P., Collaud, F., Simon-Sola, M., Charles, S., Hardet, R., et al. (2017). Rescue of Pompe disease in mice by AAV-mediated liver delivery of secretable acid α-glucosidase. Sci. Transl. Med *9*, eaam6375.

20. Raben, N., Schreiner, C., Baum, R., Takikita, S., Xu, S., Xie, T., Myerowitz, R., Komatsu, M., Van der Meulen, J.H., Nagaraju, K., et al. (2010). Suppression of autophagy permits successful enzyme replacement therapy in a lysosomal storage disorder—murine Pompe disease. Autophagy *6*, 1078–1089.

21. Ashe, K.M., Taylor, K.M., Chu, Q., Meyers, E., Ellis, A., Jingozyan, V., Klinger, K., Finn, P.F., Cooper, C.G., Chuang, W.L., et al. (2010). Inhibition of glycogen biosynthesis via mTORC1 suppression as an adjunct therapy for Pompe disease. Mol. Genet. Metab. *100*, 309–315.

22. Porto, C., Cardone, M., Fontana, F., Rossi, B., Tuzzi, M.R., Tarallo, A., Barone, M.V., Andria, G., and Parenti, G. (2009). The pharmacological chaperone N-butyldeoxynojirimycin enhances enzyme replacement therapy in Pompe disease fibroblasts. Mol. Ther. *17*, 964–971.

23. Khanna, R., Flanagan, J.J., Feng, J., Soska, R., Frascella, M., Pellegrino, L.J., Lun, Y., Guillen, D., Lockhart, D.J., and Valenzano, K.J. (2012). The pharmacological chaperone AT2220 increases recombinant human acid α-glucosidase uptake and glycogen reduction in a mouse model of Pompe disease. PLoS ONE *7*, e40776.

24. Maga, J.A., Zhou, J., Kambampati, R., Peng, S., Wang, X., Bohnsack, R.N., Thomm, A., Golata, S., Tom, P., Dahms, N.M., et al. (2013). Glycosylation-independent lysosomal targeting of acid α-glucosidase enhances muscle glycogen clearance in pompe mice. J. Biol. Chem. *288*, 1428–1438.

25. Tiels, P., Baranova, E., Piens, K., De Visscher, C., Pynaert, G., Nerinckx, W., Stout, J., Fudalej, F., Hulpiau, P., Tännler, S., et al. (2012). A bacterial glycosidase enables mannose-6-phosphate modification and improved cellular uptake of yeast-produced recombinant human lysosomal enzymes. Nat. Biotechnol. *30*, 1225–1231.

26. Biffi, A., Montini, E., Lorioli, L., Cesani, M., Fumagalli, F., Plati, T., Baldoli, C., Martino, S., Calabria, A., Canale, S., et al. (2013). Lentiviral hematopoietic stem cell gene therapy benefits metachromatic leukodystrophy. Science *341*, 1233158.

27. Biffi, A. (2017). Hematopoietic stem cell gene therapy for storage disease: current and new indications. Mol. Ther. *25*, 1155–1162.

28. van Til, N.P., Stok, M., Aerts Kaya, F.S., de Waard, M.C., Farahbakhshian, E., Visser, T.P., Kroos, M.A., Jacobs, E.H., Willart, M.A., van der Wegen, P., et al. (2010). Lentiviral gene therapy of murine hematopoietic stem cells ameliorates the Pompe disease phenotype. Blood *115*, 5329–5337.

29. Ward, N.J., Buckley, S.M., Waddington, S.N., Vandendriessche, T., Chuah, M.K., Nathwani, A.C., McIntosh, J., Tuddenham, E.G., Kinnon, C., Thrasher, A.J., and McVey, J.H. (2011). Codon optimization of human factor VIII cDNAs leads to high-level expression. Blood *117*, 798–807.

30. Bijvoet, A.G., Van Hirtum, H., Vermey, M., Van Leenen, D., Van Der Ploeg, A.T., Mooi, W.J., and Reuser, A.J. (1999). Pathological features of glycogen storage disease type II highlighted in the knockout mouse model. J. Pathol. *189*, 416–424.

31. Brazelton, T.R., Rossi, F.M., Keshet, G.I., and Blau, H.M. (2000). From marrow to brain: expression of neuronal phenotypes in adult mice. Science *290*, 1775–1779.

32. Mezey, E., and Chandross, K.J. (2000). Bone marrow: a possible alternative source of cells in the adult nervous system. Eur. J. Pharmacol. *405*, 297–302.

33. Akagi, K., Suzuki, T., Stephens, R.M., Jenkins, N.A., and Copeland, N.G. (2004). RTCGD: retroviral tagged cancer gene database. Nucleic Acids Res. *32*, D523–D527.

34. Sun, B., Zhang, H., Benjamin, D.K., Jr., Brown, T., Bird, A., Young, S.P., McVie-Wylie, A., Chen, Y.T., and Koeberl, D.D. (2006). Enhanced efficacy of an AAV vector encoding chimeric, highly secreted acid α-glucosidase in glycogen storage disease type II. Mol. Ther. *14*, 822–830.

35. Sun, B., Bird, A., Young, S.P., Kishnani, P.S., Chen, Y.T., and Koeberl, D.D. (2007). Enhanced response to enzyme replacement therapy in Pompe disease after the induction of immune tolerance. Am. J. Hum. Genet. *81*, 1042–1049.

36. Douillard-Guilloux, G., Richard, E., Batista, L., and Caillaud, C. (2009). Partial phenotypic correction and immune tolerance induction to enzyme replacement therapy after hematopoietic stem cell gene transfer of α-glucosidase in Pompe disease. J. Gene Med. *11*, 279–287.

37. Kyosen, S.O., Iizuka, S., Kobayashi, H., Kimura, T., Fukuda, T., Shen, J., Shimada, Y., Ida, H., Eto, Y., and Ohashi, T. (2010). Neonatal gene transfer using lentiviral vector for murine Pompe disease: long-term expression and glycogen reduction. Gene Ther. *17*, 521–530.

38. Ebbink, B.J., Aarsen, F.K., van Gelder, C.M., van den Hout, J.M., Weisglas-Kuperus, N., Jaeken, J., Lequin, M.H., Arts, W.F., and van der Ploeg, A.T. (2012). Cognitive outcome of patients with classic infantile Pompe disease receiving enzyme therapy. Neurology *78*, 1512–1518.

39. DeRuisseau, L.R., Fuller, D.D., Qiu, K., DeRuisseau, K.C., Donnelly, W.H., Jr., Mah, C., Reier, P.J., and Byrne, B.J. (2009). Neural deficits contribute to respiratory insufficiency in Pompe disease. Proc. Natl. Acad. Sci. USA *106*, 9419–9424.

40. Turner, S.M., Hoyt, A.K., ElMallah, M.K., Falk, D.J., Byrne, B.J., and Fuller, D.D. (2016). Neuropathology in respiratory-related motoneurons in young Pompe ($Gaa^{-/-}$) mice. Respir. Physiol. Neurobiol. *227*, 48–55.

41. Lee, K.Z., Qiu, K., Sandhu, M.S., Elmallah, M.K., Falk, D.J., Lane, M.A., Reier, P.J., Byrne, B.J., and Fuller, D.D. (2011). Hypoglossal neuropathology and respiratory activity in Pompe mice. Front. Physiol. *2*, 31.

42. Lee, N.C., Hwu, W.L., Muramatsu, S.I., Falk, D.J., Byrne, B.J., Cheng, C.H., Shih, N.C., Chang, K.L., Tsai, L.K., and Chien, Y.H. (2018). A neuron-specific gene therapy relieves motor deficits in Pompe disease mice. Mol. Neurobiol *55*, 5299–5309.

43. Hoogerbrugge, P.M., Suzuki, K., Suzuki, K., Poorthuis, B.J., Kobayashi, T., Wagemaker, G., and van Bekkum, D.W. (1988). Donor-derived cells in the central nervous system of twitcher mice after bone marrow transplantation. Science *239*, 1035–1038.

44. Cartier, N., Hacein-Bey-Abina, S., Bartholomae, C.C., Veres, G., Schmidt, M., Kutschera, I., Vidaud, M., Abel, U., Dal-Cortivo, L., Caccavelli, L., et al. (2009).

Hematopoietic stem cell gene therapy with a lentiviral vector in X-linked adrenoleukodystrophy. Science *326*, 818–823.

45. Jung, S., and Schwartz, M. (2012). Non-identical twins—microglia and monocyte-derived macrophages in acute injury and autoimmune inflammation. Front. Immunol. *3*, 89.

46. Shemer, A., and Jung, S. (2015). Differential roles of resident microglia and infiltrating monocytes in murine CNS autoimmunity. Semin. Immunopathol. *37*, 613–623.

47. Goldmann, T., Wieghofer, P., Jordão, M.J., Prutek, F., Hagemeyer, N., Frenzel, K., Amann, L., Staszewski, O., Kierdorf, K., Krueger, M., et al. (2016). Origin, fate and dynamics of macrophages at central nervous system interfaces. Nat. Immunol. *17*, 797–805.

48. Magistretti, P.J., Sorg, O., Yu, N., Martin, J.L., and Pellerin, L. (1993). Neurotransmitters regulate energy metabolism in astrocytes: implications for the metabolic trafficking between neural cells. Dev. Neurosci. *15*, 306–312.

49. Bélanger, M., Allaman, I., and Magistretti, P.J. (2011). Brain energy metabolism: focus on astrocyte-neuron metabolic cooperation. Cell Metab. *14*, 724–738.

50. Brown, A.M., Baltan Tekkök, S., and Ransom, B.R. (2004). Energy transfer from astrocytes to axons: the role of CNS glycogen. Neurochem. Int. *45*, 529–536.

51. Liang, Q., van Helsdingen, Y., van der Velden, G., Stok, M., Jacobs, E., Duncker, D., Reuser, A., van der Ploeg, A., Vulto, V., van Til, N.P., and Wagemaker, G. (2014). Lentiviral stem cell gene therapy for Pompe disease. J. Neuromuscul. Dis *2* (*Suppl 1*), S64.

52. Aiuti, A., Cassani, B., Andolfi, G., Mirolo, M., Biasco, L., Recchia, A., Urbinati, F., Valacca, C., Scaramuzza, S., Aker, M., et al. (2007). Multilineage hematopoietic reconstitution without clonal selection in ADA-SCID patients treated with stem cell gene therapy. J. Clin. Invest. *117*, 2233–2240.

53. Aiuti, A., Biasco, L., Scaramuzza, S., Ferrua, F., Cicalese, M.P., Baricordi, C., Dionisio, F., Calabria, A., Giannelli, S., Castiello, M.C., et al. (2013). Lentiviral hematopoietic stem cell gene therapy in patients with Wiskott-Aldrich syndrome. Science *341*, 1233151.

54. Hacein-Bey-Abina, S., Pai, S.Y., Gaspar, H.B., Armant, M., Berry, C.C., Blanche, S., Bleesing, J., Blondeau, J., de Boer, H., Buckland, K.F., et al. (2014). A modified γ-retrovirus vector for X-linked severe combined immunodeficiency. N. Engl. J. Med. *371*, 1407–1417.

55. Hacein-Bey-Abina, S., Von Kalle, C., Schmidt, M., McCormack, M.P., Wulffraat, N., Leboulch, P., Lim, A., Osborne, C.S., Pawliuk, R., Morillon, E., et al. (2003). LMO2-associated clonal T cell proliferation in two patients after gene therapy for SCID-X1. Science *302*, 415–419.

56. Howe, S.J., Mansour, M.R., Schwarzwaelder, K., Bartholomae, C., Hubank, M., Kempski, H., Brugman, M.H., Pike-Overzet, K., Chatters, S.J., de Ridder, D., et al. (2008). Insertional mutagenesis combined with acquired somatic mutations causes leukemogenesis following gene therapy of SCID-X1 patients. J. Clin. Invest. *118*, 3143–3150.

57. Braun, C.J., Boztug, K., Paruzynski, A., Witzel, M., Schwarzer, A., Rothe, M., Modlich, U., Beier, R., Göhring, G., Steinemann, D., et al. (2014). Gene therapy for Wiskott-Aldrich syndrome—long-term efficacy and genotoxicity. Sci. Transl. Med. *6*, 227ra33.

58. Naldini, L., Blömer, U., Gallay, P., Ory, D., Mulligan, R., Gage, F.H., Verma, I.M., and Trono, D. (1996). In vivo gene delivery and stable transduction of nondividing cells by a lentiviral vector. Science *272*, 263–267.

59. Zhang, F., Thornhill, S.I., Howe, S.J., Ulaganathan, M., Schambach, A., Sinclair, J., Kinnon, C., Gaspar, H.B., Antoniou, M., and Thrasher, A.J. (2007). Lentiviral vectors containing an enhancer-less ubiquitously acting chromatin opening element (UCOE) provide highly reproducible and stable transgene expression in hematopoietic cells. Blood *110*, 1448–1457.

60. Schambach, A., Bohne, J., Baum, C., Hermann, F.G., Egerer, L., von Laer, D., and Giroglou, T. (2006). Woodchuck hepatitis virus post-transcriptional regulatory element deleted from X protein and promoter sequences enhances retroviral vector titer and expression. Gene Ther. *13*, 641–645.

61. Cesana, D., Ranzani, M., Volpin, M., Bartholomae, C., Duros, C., Artus, A., Merella, S., Benedicenti, F., Sergi Sergi, L., Sanvito, F., et al. (2014). Uncovering and dissecting the genotoxicity of self-inactivating lentiviral vectors in vivo. Mol. Ther. *22*, 774–785.

62. Bijvoet, A.G., van de Kamp, E.H., Kroos, M.A., Ding, J.H., Yang, B.Z., Visser, P., Bakker, C.E., Verbeet, M.P., Oostra, B.A., Reuser, A.J., and van der Ploeg, A.T. (1998). Generalized glycogen storage and cardiomegaly in a knockout mouse model of Pompe disease. Hum. Mol. Genet. *7*, 53–62.

63. van Til, N.P., and Wagemaker, G. (2014). Lentiviral gene transduction of mouse and human hematopoietic stem cells. Methods Mol. Biol. *1185*, 311–319.

64. Van Leenen, D., Bijvoet, A.G., Visser, P., Heuvelsland, G.F., Verkerk, A., Van Der Horst, G.T., and Reuser, A.J. (1999). A low-cost computerized system to monitor running performance and circadian rhythms of twenty mice simultaneously. Contemp. Top. Lab. Anim. Sci. *38*, 29–32.

65. Okumiya, T., Keulemans, J.L., Kroos, M.A., Van der Beek, N.M., Boer, M.A., Takeuchi, H., Van Diggelen, O.P., and Reuser, A.J. (2006). A new diagnostic assay for glycogen storage disease type II in mixed leukocytes. Mol. Genet. Metab. *88*, 22–28.

66. Schmidt, M., Schwarzwaelder, K., Bartholomae, C., Zaoui, K., Ball, C., Pilz, I., Braun, S., Glimm, H., and von Kalle, C. (2007). High-resolution insertion-site analysis by linear amplification-mediated PCR (LAM-PCR). Nat. Methods *4*, 1051–1057.

67. van Til, N.P., de Boer, H., Mashamba, N., Wabik, A., Huston, M., Visser, T.P., Fontana, E., Poliani, P.L., Cassani, B., Zhang, F., et al. (2012). Correction of murine *Rag2* severe combined immunodeficiency by lentiviral gene therapy using a codon-optimized *RAG2* therapeutic transgene. Mol. Ther. *20*, 1968–1980.

68. de Waard, M.C., van der Velden, J., Bito, V., Ozdemir, S., Biesmans, L., Boontje, N.M., Dekkers, D.H., Schoonderwoerd, K., Schuurbiers, H.C., de Crom, R., et al. (2007). Early exercise training normalizes myofilament function and attenuates left ventricular pump dysfunction in mice with a large myocardial infarction. Circ. Res. *100*, 1079–1088.

OMTM, Volume *17*

Supplemental Information

Lentiviral Hematopoietic Stem Cell Gene Therapy Corrects Murine Pompe Disease

Merel Stok, Helen de Boer, Marshall W. Huston, Edwin H. Jacobs, Onno Roovers, Trudi P. Visser, Holger Jahr, Dirk J. Duncker, Elza D. van Deel, Arnold J.J. Reuser, Niek P. van Til, and Gerard Wagemaker

S1 Fig. Circadian rhythm is maintained in voluntary running wheel exercises.

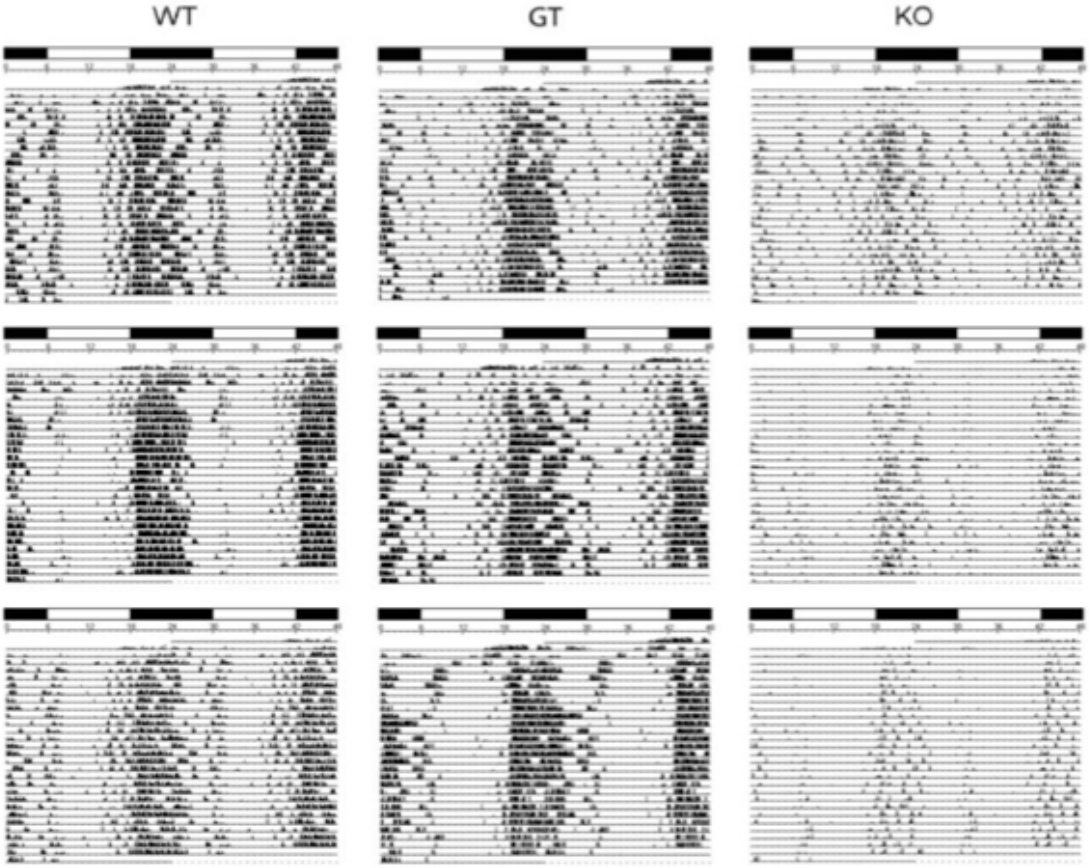

The actograms represent circadian locomotor activity and rest cycles. The interrupted horizontal bar above the actograms displays day (white) and night (black) cycles. A 48-hour time frame is shown depicting running periods (in black) and resting periods out of the running wheels. Three representative mice are displayed for each condition, i.e. wild-type (WT), *GAAco* treated *Gaa*$^{-/-}$ mice (GT) and *Gaa*$^{-/-}$ mice (KO). All animals became more active during the night and all groups showed similar day/night activity patterns, except that KO mice were considerably less active.

S2 Fig. GAA in microglia (upper panel, magnification x 100) and astrocytes (magnification x 10).

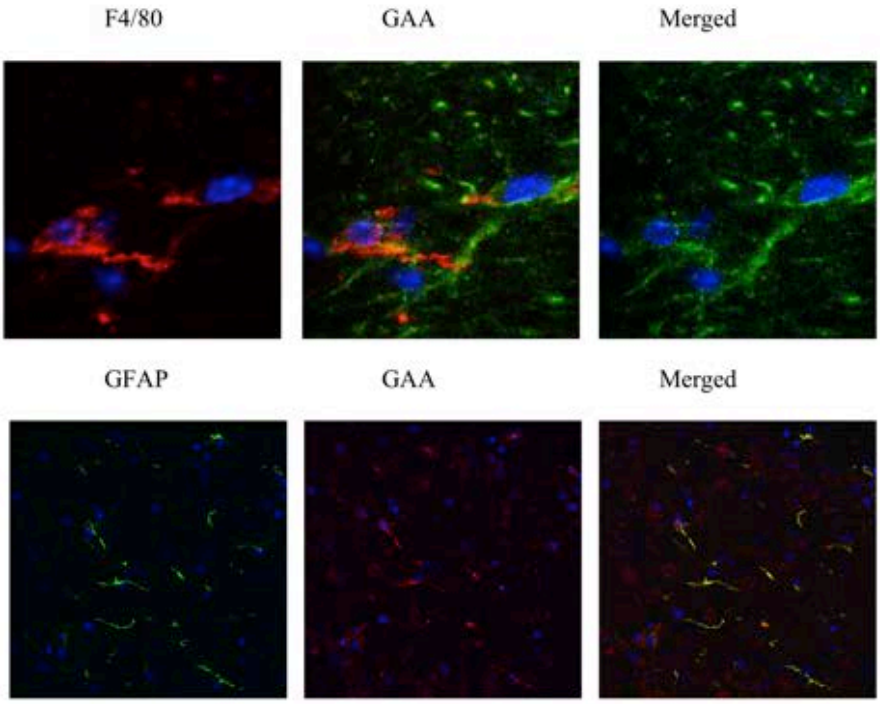

Representative areas of microglia with in green the GAA staining and in red the F4/80 staining, whereas blue represents the Hoechst staining. In the astrocytes, red represents GAA staining and green the astrocytes GFAP staining, showing that virtually all astrocytes stain positive for GAA.

S1 Table. Common integration sites

Vector	Num. of samples	Total IS	Unique Genes	IS within 10kb of TSS	IS within 10kb of gene	Intronic IS
GAAco	36	333	310	65	221	180
GFP	5	424	388	91	304	249
Continuation:						
Unique Oncogenes	Total oncogenes	CIS	CIS oncogenes	Frequency oncogenes	Frequency intronic IS	Frequency IS w/in 10kb of gene
12	14	15	2	4.2%	54.1%	66.4%
12	13	25	1	3.1%	58.7%	71.7%

S2 Table. List of all CIS, oncogenes in red

vector	CISorder	Chromsome	Gene	Loci
GAAco	2	1	Cr2	197025311;197025462
GAAco	2	8	Eps15l1	74919901;74919904
GAAco	2	X	Cybb	9041400;9041771
GAAco	2	1	Smap1	23885960;23885961
GAAco	2	1	37500	95387308;95387315
GAAco	2	1	Mcm6	130277570;130277585
GAAco	2	1	Scarna3a	161234959;161234977
GAAco	2	1	Gm4846	168411650;168411781
GAAco	2	1	Cr1l	196946840;196946841
GAAco	2	9	Trpc6	8581308;8581617
GAAco	2	9	Elovl5	77797454;77797462
GAAco	2	10	Mir1929	44061578;44061740
GAAco	2	10	Ascc3	50315191;50315792
GAAco	2	16	Mir28	24902396;24902457
GAAco	2	18	Tmx3	90693725;90712409
GFP	2	18	Zfp521	13872964;13873209
GFP	2	2	Plxdc2	16282665;16282854
GFP	2	3	Gyg	20021989;20022410
GFP	2	3	Hist2h2aa2	96047653;96048217
GFP	2	3	Sfrs11	157683042;157707831
GFP	2	5	Pcdh7	58178866;58187690
GFP	2	5	Cenpc1	86387408;86387768
GFP	2	5	AU042671	121751014;121751172
GFP	2	6	Cul1	47445391;47464266
GFP	2	6	Bicd1	149497766;149508206
GFP	2	8	Large	75821352;75821490
GFP	2	9	Slc37a2	37102871;37103208
GFP	2	10	Jmjd1c	66660521;66689907
GFP	2	11	Sfi1	3086225;3095580
GFP	2	11	Slfn1	82909694;82925619
GFP	2	11	H3f3b	115887991;115888197
GFP	2	12	Stxbp6	46220785;46221361
GFP	2	13	Hrh2	54307859;54308041
GFP	2	13	Edil3	89376126;89376754
GFP	2	15	Abra	41616255;41616522
GFP	2	15	Taf2	54871080;54871277
GFP	2	15	Phf20l1	66402373;66402700
GFP	2	16	Cggbp1	64821368;64821516
GFP	2	16	Gbe1	70413892;70418655
GFP	2	18	Wac	7873989;7901856